

Graphene for next generation magnetic devices: A first-principles study

Pranay Ranjan^{1#}, Atif Sattar^{1#}, Maamar Benkraouda¹, Slaven Garaj², Nouredine Amrane^{1*}, El-Hadi S. Sadki^{1*}

¹Department of Physics, United Arab Emirates University, Al-Ain, UAE

²Department of Physics, National University of Singapore, Singapore 117542, Singapore

[#]Equal first author contribution

*Corresponding Authors: namrane@uaeu.ac.ae, e_sadki@uaeu.ac.ae

Abstract—Graphene, an atomic thin sheet of monolayer carbon atoms, is deemed to replace silicon and revolutionize the electronics industry. It has massless Dirac fermions and exhibits ballistic charge transport, a prerequisite for upcoming futuristic nanodevices, such as field-effect transistors, sensors, etc. However, it lacks an intrinsic electronic bandgap and thus is obsolete for use in these applications. In this work, a first principles study is used to predict the opening of a bandgap in graphene by an engineered introduction of modulations in its lattice. Moreover, it is found that the atomic modulation and the addition of hydrogen atoms at sub-lattices induce magnetism in the graphene sheets. The hydrogen-induced itinerant magnetism (ferromagnetic or antiferromagnetic) depends on the type of defects and the structure of the sheet. This hydrogen-induced spin promotes the role of graphene as a potential material for magnetic memory device applications. Furthermore, with the creation of atomic vacancies and quasilocalized states, it is deemed to allow selective permeation (water/gas) and thus paves the way for its use in-filtration (membrane technology) and hydrogen storage applications.

Keywords—Graphene, Spintronics, magnetic devices, first-principles study

I. INTRODUCTION

Graphene, discovered by Novoselov and Geim in 2004 [1], is one of the most fascinating materials due to its unprecedented physical and chemical properties, such as high conductivity, electron mobility, observation of quantum Hall effect at room temperature, ballistic transport of charge carriers, layer dependent bandgap, and high mechanical strength [1-7]. Graphene-based magnetic devices have recently been the centre of attraction for memory storage device applications [8-15]. This generated strong interest in the scientific community to explore methods for inducing magnetism in graphene as carbon atoms themselves don't possess any intrinsic magnetic moment. Among these methods are edge (zigzag and armchair) modification, hydrogen atoms adsorption, and creation of defects in sub-lattices [8-21] (see Fig. 1.).

Graphene's paradigm of magnetism revolves around two widely accepted concepts. The first model is based on graphene zigzag edge topologies nanosheets and ribbons called nanographene (NG) or graphene nanoribbons (GNRs), which are deemed to have low-energy edge-localized states [22-25].

Increase in graphene sheet size causes edge-localized states to reach near the Fermi-level, and thus Coulombic repulsion can be observed between valence bands, which causes spin polarization. The second model, and the conceptually easier to understand, includes an imbalance between the sub-lattices in the bipartite graphene lattice, which according to Lieb's theorem, makes a spin imbalance in the sheet [26]. This can be realized via the creation of mono, bi or tri vacancies that remove a P_z orbital on graphene sheets, or by a specific change in NGs where the sub-lattice imbalance is structurally inherent, so that typical classical Kekulé structure (where an alternating single is followed by double bonds) cannot be assigned [25-26]. Moreover, defects induce a spin degree of freedom to the electrons and trigger spintronics in graphene sheets. Graphene has promising spin transport properties at room temperature, and is being deemed to be the best-suited material for spintronics, including gate-tunable carrier concentration and high electronic mobility [24-25]. Spintronics in graphene sheets is promising for application in information storage and logic devices. Hence, the demand for high speed, low power consumption, high conductivity and mobility of electrons in spin transistors for reconfigurable logic gates could be readily addressed.

In this work, by using first-principles calculations, we demonstrate an efficient way to inject magnetic moments in graphene by controlled vacancy defects, with a more realistic approach so that it can be experimentally achievable. Furthermore, the injection of spin-polarized carriers into graphene by introducing hydrogen atoms has been analysed from a theoretical perspective. An investigation of the spin lifetimes and the spin diffusion length properties in graphene have been conducted, and compared with other metals and semiconductors. Finally, upcoming graphene-based futuristic devices have been summarized.

II. BANDGAP ENGINEERING IN GRAPHENE

The difference in bandgap between graphene, graphite and graphane attests the possibility of tailoring the bandgap of graphene. The opening of a bandgap may be realized by mono- or bi- vacancies, atomic defects, through zigzag or edge effects,

topological frustration, or through induced functionalization in the graphene sheet (Fig. 1). The latter endows them with a large bandgap due to transformation of hybridization state of carbon atoms from sp^2 to sp^3 . Recently, a functional group, such as hydrogen on one side of the graphene sheet, was theoretically explored along with mono or bi-atomic vacancy via first-principles calculations, and was also supported by experimental observations by Elias et al. [27]. It was found that hydrogenation of graphene (plasma-oriented atomic hydrogen) changes the bandgap and can be controlled by adsorption or desorption of hydrogen atoms. Moreover, Balog et al. [28] reported that if hydrogen gets adsorbed onto a Moiré superlattice pattern it can lead to the opening of a bandgap in the range of ~ 0.45 eV. As defects are induced, or hydrogen atoms are adsorbed, a midgap region (also known as Midstate) is induced in the graphene sheet through the creation of one unpaired local π electron (or radical). It was also predicted to lead to a large magnetic-coupling strength in comparison to pristine graphene sheets. However, inducing systematically a tunable bandgap

and magnetism in graphene sheets remains to be discovered.

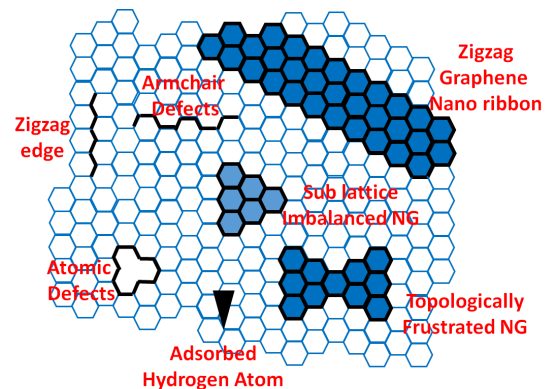


Fig. 1. Schematic diagram depicting types of defects that lead to the opening of a bandgap in monolayer atomic graphene sheet

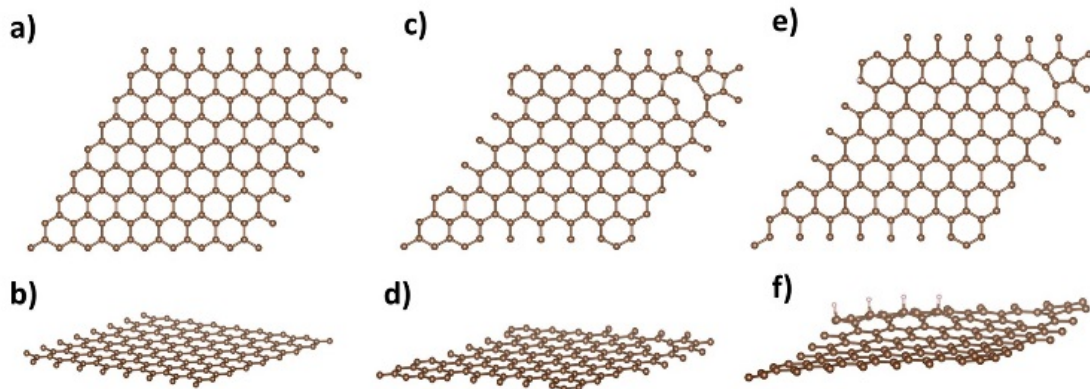


Fig. 2. Top view (a), (c), (e) and side view (b), (d), (f) of graphene sheets, defect induced graphene sheets and defect along with hydrogen atoms in the graphene sheet, respectively.

III. STRUCTURAL AND COMPUTATIONAL DETAILS

Graphene, a monolayer sheet of carbon atoms arranged in a honeycomb pattern is a semi-metallic 2D sheet with a zero bandgap. Interestingly, it has the highest conductivity, mobility, thermal and mechanical strength amongst all 2D materials. However, it fails to deliver the promise it upholds for electronics industry due to its zero bandgap. In graphene, the conduction band and valence band touch each other at two different points, namely K and K_0 . To avoid any errors and to ensure the accuracy of our calculations, we made a relatively large supercell of $8 \times 8 \times 1$ sheet of graphene (Fig. 2 (a)) in the simulations. Once the optimized sheet lattice structure and band structure for graphene is obtained and a zero bandgap is obtained (see results section) then we proceed with the calculation of defects and hydrogen atoms adsorbed on graphene sheets (Fig. 2 (b & c)). It

is to be noted that all the optimized structures as well as band structure calculations for graphene sheets, without adding or modifying its structure, is in agreement with the theoretical results reported elsewhere, and thus confirms the accuracy and reliability of our calculations.

Computational details used for graphene (with/without/hydrogen attached) sheets calculations were done by first-principles Density Functional Theory (DFT) in the plane-wave basis using Vienna Ab-initio Simulation Package (VASP) [29]. The projected augmented wave (PAW) pseudopotentials [30] along with generalized gradient approximation (GGA) of Perdew, Burke, and Ernzerhof (PBE) were used for the exchange-correlation energy [31].

Superlattices geometry optimizations were carried out using the conjugate energy scheme until each atom force components came to less than 0.01 eV/Å.

The convergence criterion for total energy was calibrated to 10^{-5} eV in the self-consistent field (SCF) iteration. The optimized and relaxed structures were taken to compute the density of states (DOS) and electronic band structures.

IV. RESULTS AND DISCUSSIONS

The magnetic moment in graphene seems to be an illusive dream, as it does not consist of any *d*- or *f*-electrons unless it is induced by defects. Practically, inducing magnetism naturally can give rise to high Curie-temperature with diluted magnetism but it can meet the ever-growing demand for magnetic storage

moment can be understood by Lieb's bipartite lattice. Considering the case of graphene sheets, the magnetic moment of the ground state is $\mu_B = |N_A - N_B|$, where μ_B is the Bohr magneton, N_A and N_B are the sublattices sites [24]. Removal of a single atom or by addition of any hydrogen atom at the sublattices can lead to the formation of a magnetic moment in the π band. Accordingly, we have created defects in the graphene sheet, and their band structures, as well as density of states, are presented in Fig. 3(b & e) and defect induced graphene sheet along with attached hydrogen atoms are presented in Fig. 3(c & f), respectively. In the electronic band structure plots, the solid yellow lines represent the spin-up channel and the blue

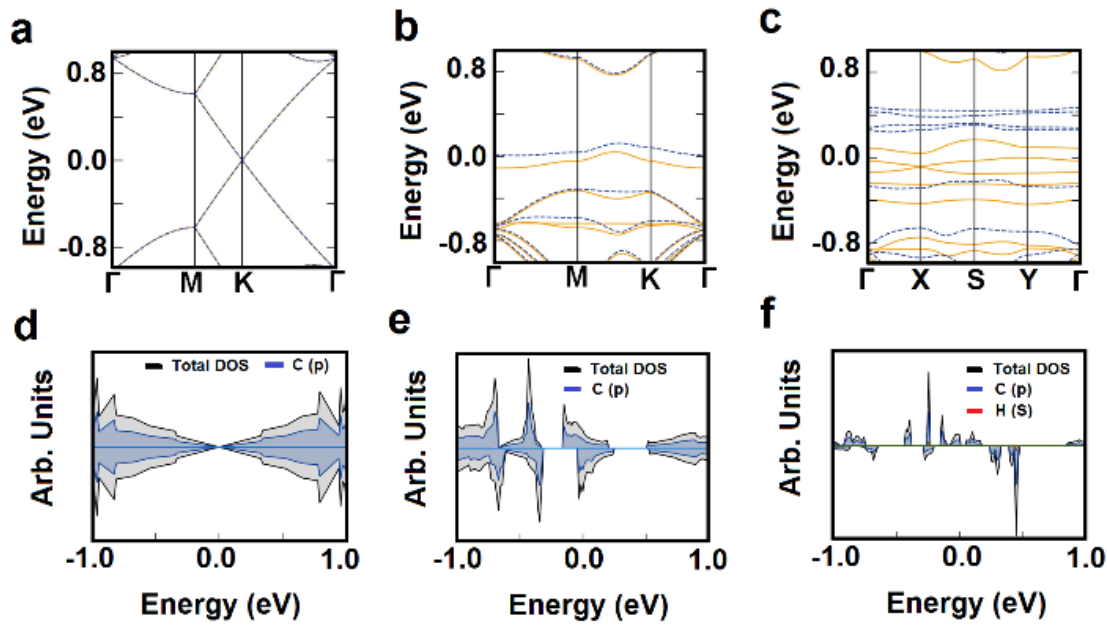




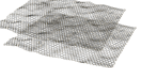
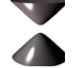
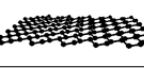

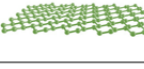

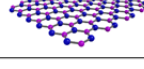

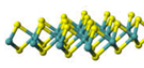

Fig. 3. Spin-polarized band structures of (a) pristine graphene, (b) graphene with a defect and (c) graphene with a defect and an attached hydrogen atom, with their corresponding density of states in (d), (e) and (f) respectively.

devices at an atomistic level using 2D materials. Pristine graphene sheets are completely diamagnetic and have a zero bandgap as illustrated with its band structure in Fig. 3(a). It can be seen that valance band maxima and conduction band minima are almost touching each other at the Fermi level, $E_F = 0$ eV, at the K-point of the first Brillion zone. The spin-polarized density of states (DOS) of the pristine graphene presented in Fig. 3(d) exhibits its non-magnetic, metallic property. The *p*-states of the carbon atom are symmetrical and equally distributed in both spin-up and spin-down channels. The next big question is, how to induce magnetic order and to get control over it. Also, what should be the first step is a discussion of vital importance. The most suitable answer seems to be an induced tunable magnetism in graphene which can be controlled by a potential, doping, defects, or by chemical functionalization. Theoretical explanation of the existence of magnetic

dashed-lines denotes the spin-down channel. Prominent splitting of *p*-states of carbon (denoted by the letter C in the figures) near the Fermi level ($E_F = 0$ eV) can be observed from the band structures of the defected graphene, as well as from the DOS plots in the defect induced graphene sheet (Fig. 3(b & e)), and for the defect and hydrogen attached graphene sheet (Fig. 3(c & f)). It is evident from the electronic properties that the defect-induced graphene sheet is metallic in both spin-up and spin-down channels, and magnetism of $\sim 1.39\mu_B$ is induced due to the single vacancy.

Inducing a single vacancy in graphene sheets will initiate local spin-polarized electronic-density through the removal of the four electrons from the bands. Out of the four electrons, three of the electrons from the dangling bonds (sp^2 , σ bonds) gets split due to the Jahn-Teller distortion or by the crystal field [24]. Moreover, the Fermi sea gets a double occupancy, while one close to the Fermi level will get singly occupied, thus creating $1\mu_B$ magnetic moment. According to the Lieb's theorem, π -state generates $1\mu_B$ magnetic moment and by using Hund's coupling for the singly occupied σ - and π -states, the total moment can be approximated to $2\mu_B$. However, in

Table 1. Summary of the upcoming 2D materials band structures at K and Γ points.

Material	Structure	Spectrum at K	Δ_K	Δ_Γ
Graphene [34-36]			24 μeV –50 μeV	8.8 meV
Bi-layer Graphene [37]			24 μeV	8.6 meV
Silicene [38]			1.6 meV	33.7 meV
Germanene [38]			24 meV	195 meV
Boron nitride [39]			30 μeV 15 μeV	12.6 meV
Molybdenum Disulphide [40-41]			3 meV 147 meV	0

first-principles calculations, using density functional theory, this gets reduced to $\sim 1.7\mu_B$ due to polarization of the itinerant π -band. It has been observed that Fermi level shifting is difficult to observe via the inclusion of mono vacant sites in graphene sheets. Therefore, it can be inferred that the goal to induce magnetism can be achieved only by switching off the resonant π part of the vacancy moments states. Finally, one can infer that it is difficult to predict magnetism via isolated vacancy in graphene [32]. Our next step was to induce a controllable magnetism via the introduction of a hydrogen atom as it forms a covalent bond with carbon, thus, removes the P_z orbital and enables sublattice mismatch or imbalance. In accordance with Lieb's theorem, the addition of a single hydrogen atom will induce a resonant state having a magnetic moment $1\mu_B$. As we have already tuned the magnetic moment by inducing a mono vacancy. Therefore, we tried to induce a strong but controllable magnetic behaviour by introducing three hydrogen atoms along with the defect. In short, we induced $3\mu_B$ because the addition of more hydrogen atoms will influence the ground state and seems to be impossible to measure spin spiral [33]. On the other hand, 100% spin-polarization has been achieved in the hydrogen attached defected graphene with a magnetic moment of exactly $4\mu_B$. The hydrogen attached to the defect induced graphene sheet exhibits half-metallic (HM) ferromagnetism. In the spin-up channel it shows metallic behaviour, while in the spin-down channel, it has a bandgap of 0.62 eV, which confirms the HM ferromagnetic property of the sheet leading to the 100% spin polarization at the Fermi level E_F .

The spin-orbit gaps Δ_K at K (Fermi level) and Δ_Γ at Γ points of the Brillouin zone govern the magnetic property and spintronics in 2D materials, we,

therefore, summarized the values of selected new 2D materials in Table 1, which appears to be suitable for magnetic devices. It was found that in the case of monolayer graphene sheet the spin-orbit splitting at the Γ point is observed at 8.8 meV and is attributed to the carbon spin-orbit coupling [34-36]. Also, the Dirac cone formation by the hybridization of the P_z orbitals at K point, and the spin-orbit splitting appears to be very small for monolayer graphene sheet and is in the range of 24–50 μeV [34–36]. Contrary to graphene (monolayer or bilayer), other metallic 2D materials, such as silicene and germanene, appear to be more suitable in exhibiting spin-orbit effects, due to the presence of larger values of spin-orbit couplings [38-39]. Moreover, in comparison to metallic 2D sheets, insulating as well as semiconducting 2D materials, such as h-BN and MoS₂, exhibit weak spin-orbit couplings [39-41].

Defect in graphene sheets is also seen as pores in water filtration technology and the pore size determines the rate of water flux. Cohen-Tanugi and Grossman [42] have examined the optimal pore size for water filtration using classical molecular dynamics simulations and have calculated the optimal value of pores to be 5.5 Å. However, a pore size greater than 5.5 Å, can also be used as a suitable membrane for water filtration technology if functional groups can be added to the edges of defect sites. It was found that out of several existing functional group such as aldehyde, ketone, carboxyl, ether etc. the introduction of H-atom is the most suitable for water filtration, as the H-atoms rim forces an extra conformational order of flow, in which the curtailment by the H-bonding allows a more robust salt rejection. This unique structure of graphene with hydrogen and defect has interestingly potential applications in many other

fields such as electronic applications at room temperature [28], water filtration and desalination [42], hydrogen storage [43], etc.

V. CONCLUSION

Our first-principles calculations reveal that magnetism can be induced in graphene sheets that have atomic vacancies and/or adsorbed hydrogen atoms. A single atomic vacancy on the graphene sheet leads to metallic properties in both spin channels with a magnetic moment of $1.39\mu_B$. Half-metallic ferromagnetism is found when graphene with a mono-vacancy is attached with a hydrogen atom. The observed total magnetic integral moment of $4\mu_B$ is a very promising result for spintronics applications. The designed graphene sheet with anchored functionalization is also predicted to be a suitable candidate for water filtration and desalination applications.

ACKNOWLEDGMENT

This work was supported by a United Arab Emirates University-Asian Universities Alliance (UAEU-AUA) Joint Research Project (Grant Number 31R196) and a United Arab University Program for Advanced Research (UPAR) Grant (Number 31S360).

REFERENCES

- [1] K. S. Novoselov, A. K. Geim, S. V. Morozov, D. Jiang, Y. Zhang, S. V. Dubonos, I. V. Grigorieva, A. A. Firsov, "Electric field effect in atomically thin carbon films," *Science*, vol. 306, pp. 666, October 2004.
- [2] A.K. Geim, K. S. Novoselov, "The rise of graphene," *Nat. Mater.*, vol. 6, pp. 183, March 2007.
- [3] K. Geim, "Graphene: Status and Prospects," *Science*, vol. 324, pp. 1530, June 2009.
- [4] H. Castro Neto, F. Guinea, N. M. R. Peres, K. S. Novoselov, A. K. Geim, "The electronic properties of graphene," *Rev. Mod. Phys.*, vol. 81, pp. 109, January 2009.
- [5] J.-H. Chen, C. Jang, S. Xiao, M. Ishigami, M. S. Fuhrer, "Intrinsic and extrinsic performance limits of graphene devices on SiO₂," *Nat. Nanotechnol.*, vol. 3, pp. 206, March 2008.
- [6] Meric, M. Y. Han, A. F. Young, B. Ozyilmaz, P. Kim, K. L. Shepard, "Current saturation in zero-bandgap, top-gated graphene field-effect transistors," *Nat. Nanotechnol.*, vol. 3, pp. 654, september 2008.
- [7] A. A. Balandin, S. Ghosh, W. Bao, I. Calizo, D. Teweldebrhan, F. Miao, C. N. Lau, "Superior Thermal Conductivity of Single-Layer Graphene," *Nano Lett.*, vol. 8, pp. 902, February 2008.
- [8] M. Y. Han, B. Ozyilmaz, Y. Zhang, P. Kim, "Energy Band-Gap Engineering of Graphene Nanoribbons," *Phys. Rev. Lett.*, vol. 98, pp. 206805, March 2007.
- [9] T. G. Pedersen, C. Flindt, J. Pedersen, N. A. Mortensen, A.-P. Jauho, K. Pedersen, "Graphene Antidot Lattices: Designed Defects and Spin Qubits," *Phys. Rev. Lett.*, vol. 100, pp. 136804, April 2008.
- [10] A. Yan, L. Xian, M. Y. Chou, "Structural and Electronic Properties of Oxidized Graphene," *Phys. Rev. Lett.*, vol. 103, pp. 086802, August 2009.
- [11] O. Sofo, A. S. Chaudhari, G. D. Barber, "Graphane: A two-dimensional hydrocarbon," *Phys. Rev. B*, vol. 75, pp. 153401, April 2007.
- [12] M. Pereira, A. H. Castro Neto, "Strain Engineering of Graphene's Electronic Structure," *Phys. Rev. Lett.*, vol. 103, pp. 046801, July 2009.
- [13] Jacoboni, C. Canali, G. Ottaviani, A. A. Quaranta, "A review of some charge transport properties of silicon," *Solid-State Electron.* Vol. 20, pp. 77, February 1977.
- [14] M. Pereira, A. H. Castro Neto, N. M. R. Peres, "Tight-binding approach to uniaxial strain in graphene," *Phys. Rev. B*, vol. 80, pp. 045401, July 2009.
- [15] G. Gui, J. Li, J. Zhong, "Band structure engineering of graphene by strain: First-principles calculations," *Phys. Rev. B*, vol. 80, pp. 167402, August 2008.
- [16] S.-M. Choi, S.-H. Jhi, Y.-W. Son, "Effects of strain on electronic properties of graphene," *Phys. Rev. B*, vol. 81, pp. 081407, February 2010.
- [17] Naumov, A. M. Bratkovsky, "Gap opening in graphene by simple periodic inhomogeneous strain," *Phys. Rev. B*, vol. 84, pp. 245444, December 2011.
- [18] G. Kresse, J. Furthmüller, "Efficiency of ab-initio total energy calculations for metals and semiconductors using a plane-wave basis set," *Comput. Mater. Sci.*, vol. 6, pp. 15, July 1996.
- [19] G. Kresse, J. Furthmüller, "Efficient iterative schemes for ab initio total-energy calculations using a plane-wave basis set," *Phys. Rev. B*, vol. 54, pp. 11169, October 1996.
- [20] P. E. Blochl, "Projector augmented-wave method," *Phys. Rev. B*, vol. 50, pp. 17953, December 1994.
- [21] G. Kresse, D. Joubert, "From ultrasoft pseudopotentials to the projector augmented-wave method," *Phys. Rev. B*, vol. 59, pp. 1758, January 1999.
- [22] Nakada, K., Fujita, M., Dresselhaus, G. & Dresselhaus, M. S. "Edge state in graphene ribbons: nanometer size effect and edge shape dependence," *Phys. Rev. B* vol. 54, pp. 17954–17961, December 1996.
- [23] Fernández-Rossier, J. J. Palacios, "Magnetism in graphene nanoislands," *Phys. Rev. Lett.*, vol. 99, pp. 177204, October 2007.
- [24] W. Han, R. K. Kawakami, M. Gmitra, J. Fabian, "Graphene Spintronics," *Nature Nanotechnology*, vol. 9, October 2014.
- [25] P. Ruffieux, et al., "On-surface synthesis of graphene nanoribbons with zigzag edge topology," *Nature*, vol. 531, pp. 489–492, March 2016.
- [26] E. H. Lieb, "Two theorems on the Hubbard model," *Phys. Rev. Lett.*, vol. 62, pp. 1201–1204, March 1989.
- [27] C. Elias, R. R. Nair, T. M. G. Mohiuddin, S. V. Morozov, P. Blake, M. P. Halsall, A. C. Ferrari, D. W. Boukhvalov, M. I. Katsnelson, A. K. Geim, K. S. Novoselov, "Control of Graphenes Properties by Reversible Hydrogenation: Evidence for Graphane," *Science*, vol. 323, pp. 610, January 2009.
- [28] R. Balog, B. Jørgensen, L. Nilsson, M. Andersen, E. Rienks, M. Bianchi, M. Fanetti, E. Lagsgaard, A. Baraldi, S. Lizzit, Z. Slijivancanin, F. Besenbacher, B. Hammer, T. G. Pedersen, P. Hofmann, L. Hornekaer, "Bandgap Opening in Graphene Induced by Patterned Hydrogen Adsorption," *Nat. Mater.*, vol. 9, pp. 315, March 2010.
- [29] G. Kresse, J. Furthmüller, "Efficient iterative schemes for ab initio total-energy calculations using a plane-wave basis set," *Phys. Rev. B*, 54, 16, 11169, 1994.
- [30] P.E. Blöchl, "Projector augmented-wave method," *Phys. Rev. B*, vol. 50, pp. 17953, October 1994.
- [31] M. Ernzerhof, G. E. Scuseria, "Assessment of the Perdew–Burke–Ernzerhof of exchange-correlation functional," *J. Chem. Phys.* Vol. 110, pp. 5029, March 1999.
- [32] J. J. Palacios, F. Ynduráin, "Critical analysis of vacancy-induced magnetism in monolayer and bilayer graphene," *Phys. Rev. B*, vol. 85, pp. 245443, June 2012.
- [33] A. N. Rudenko, F. J. Keil, M. I. Katsnelson, A. I. Lichtenstein, "Exchange interactions and frustrated magnetism in single-side hydrogenated and fluorinated graphene," *Phys. Rev. B*, vol. 88, pp. 081405, June 2013.
- [34] M.Gmitra, S. Konschuh, C. Ertler, C. Ambrosch-Draxl, J. Fabian, "Band-structure topologies of graphene: Spin-orbit coupling effects from first principles," *Phys. Rev. B*, vol. 80, pp. 235431, December 2009.
- [35] S. Abdelouahed, A. Ernst, J. Henk, I. V. Maznichenko, I. Mertig, "Spin-split electronic states in graphene: Effects due to lattice deformation, Rashba effect, and adatoms by first principles," *Phys. Rev. B*, vol. 82, pp. 125424, September 2010.

- [36] J. C. Boettger, S. B. Trickey, "First-principles calculation of the spin-orbit splitting in graphene," *Phys. Rev. B*, 75, 121402, 2007.
- [37] S. Konschuh, M. Gmitra, D. Kochan, J. Fabian, "Theory of spin-orbit coupling in bilayer graphene," *Phys. Rev. B*, vol. 85, pp. 115423, March 2012.
- [38] C.-C. Liu, W. Feng, Y. Yao, "Quantum spin Hall effect in silicene and two-dimensional germanium," *Phys. Rev. Lett.*, vol. 107, pp. 076802, August 2011.
- [39] X. Blase, A. Rubio, S. G. Louie, M. L. Cohen, "Quasiparticle band structure of bulk hexagonal boron nitride and related systems," *Phys. Rev. B*, vol. 51, pp. 6868–6875, March 1995.
- [40] D. Y. Qiu, F. H. da Jornada, S. G. Louie, "Optical spectrum of MoS₂: Many-body effects and diversity of exciton states," *Phys. Rev. Lett.*, vol. 111, pp. 216805, November 2013.
- [41] K. Kořmider, J. W. González, J. Fernández-Rossier, "Large spin splitting in the conduction band of transition metal dichalcogenide monolayers," *Phys. Rev. B*, vol. 88, pp. 245436, December 2013.
- [42] D. Cohen-Tanugi, J. C. Grossman, "Water desalination across nanoporous graphene," *Nano Lett.*, vol. 12, pp. 3602–3608, January 2012.
- [43] M. Ye, Z. Zhang, Y. Zhao, L. Qu, "Graphene Platforms for Smart Energy Generation and Storage," *Joule* vol. 2, pp. 245–268, February 2018.